Novel Properties of Tyrosine-mutant AAV2 Vectors in the Mouse Retina

Hilda Petrs-Silva[1], Astra Dinculescu[1], Qiuhong Li[1], Wen-Tao Deng[1], Ji-jing Pang[1], Seok-Hong Min[2], Vince Chiodo[1], Andy W Neeley[1], Lakshmanan Govindasamy[3,4], Antonette Bennett[3,4], Mavis Agbandje-McKenna[3–5], Li Zhong[6], Baozheng Li[7], Giridhara R Jayandharan[5,7], Arun Srivastava[5,7,8], Alfred S Lewin[8] and William W Hauswirth[1]

[1]Department of Ophthalmology, University of Florida, Gainesville, Florida, USA; [2]Bikam Pharmaceuticals Inc., Alachua, Florida, USA; [3]Department of Biochemistry, University of Florida, Gainesville, Florida, USA; [4]Department of Molecular Biology, University of Florida, Gainesville, Florida, USA; [5]Powell Gene Therapy Center, University of Florida, Gainesville, Florida, USA; [6]Gene Therapy Center, University of Massachusetts Medical School, Worcester, Massachusetts, USA; [7]Division of Cellular and Molecular Therapy, Department of Pediatrics, University of Florida, Gainesville, Florida, USA; [8]Department of Molecular Genetics & Microbiology, University of Florida, Gainesville, Florida, USA

Vectors based on adeno-associated virus serotype 2 (AAV2) have been used extensively in many gene-delivery applications, including several successful clinical trials for one type of Leber congenital amaurosis in the retina. Many studies have focused on improving AAV2 transduction efficiency and cellular specificity by genetically engineering its capsid. We have previously shown that vectors-containing single-point mutations of capsid surface tyrosines in serotypes AAV2, AAV8, and AAV9 displayed significantly increased transduction efficiency in the retina compared with their wild-type counterparts. In the present study, we evaluated the transduction characteristics of AAV2 vectors containing combinations of multiple tyrosine to phenylalanine mutations in seven highly conserved surface-exposed capsid tyrosine residues following subretinal or intravitreal delivery in adult mice. The multiply mutated vectors exhibited different *in vivo* transduction properties, with some having a unique ability of transgene expression in all retinal layers. Such novel vectors may be useful in developing valuable new therapeutic strategies for the treatment of many genetic diseases.

Received 5 March 2010; accepted 29 September 2010; published online 2 November 2010. doi:10.1038/mt.2010.234

INTRODUCTION

Adeno-associated virus type 2 (AAV2) has been the most extensively studied of the 12 different AAV serotypes currently characterized.[1] Recombinant vectors based on AAV2 have been widely used for gene therapy applications in animal models and human clinical trials.[2] In the retina, several recent clinical trials involving treatment of one form of Leber congenital amaurosis, have shown that AAV2 can be used to deliver a complementary DNA encoding the normal 65 kda retinal pigment epithelium protein (RPE65) to humans with recessive RPE65 mutations, leading to vision improvement.[3–6] Conventional AAV vectors carry a linear, single-stranded DNA genome containing the therapeutic transgene and promoter flanked by palindromic inverted terminal repeat sequences. The 60-subunit icosahedral AAV2 capsid is assembled from three overlapping viral proteins VP1 (87 kd), VP2 (73 kd), and VP3 (62 kd), encoded by the cap gene, in a predicted ratio of 1:1:10. The three VP capsid proteins share a common C-terminal sequence, with VP1 containing a unique N-terminal region of 138 amino acids (VP1u). VP3 is the most abundant AAV2 capsid protein, comprising ~90% of its structure. The available crystal structure of AAV2 is ordered from amino acid 217 to 735 (VP1 numbering) within the VP3 common region, thus defining the minimal VP requirements for capsid assembly. The VP1u and the N-terminal regions of VP2 (65aa) and VP3 (14aa) are not ordered, but predicted to be located inside the capsid.[7,8]

The cell surface heparan sulfate proteoglycan is the primary viral receptor for AAV serotype 2.[9] Several positively charged residues, including R484, R487, K527, K532, R585, and R588 of AAV2 have been implicated in heparin binding.[10,11] In addition, coreceptors such as human fibroblast growth factor receptor 1, integrins $\alpha_v\beta_5$ and $\alpha5\beta1$, 37/67 kd laminin receptor, and hepatocyte growth factor receptor, have also been proposed to interact with AAV2 at the cell surface and modulate internalization and transduction efficiency.[12–16] Although AAV2 vectors can transduce a variety of cell types and tissues, the onset of gene expression is slow and they typically require several weeks to achieve sustained, steady-state levels of transgene expression.[17,18] Other serotypes such as AAV8 provide higher levels of transgene expression more quickly than AAV2 in liver,[19] retina,[17] and the brain.[20] The AAV capsid has been reported to influence the transduction efficiency at many steps, including vector binding to cell surface receptors, internalization, cytoplasmic trafficking to the nuclear membrane, and viral uncoating.[21] It has been shown that epidermal growth factor receptor protein tyrosine kinase-mediated phosphorylation of capsid

The first two authors contributed equally to this work.

Correspondence: *Astra Dinculescu, Department of Ophthalmology, University of Florida, 1600 SW Archer Road, Gainesville, Florida 32610-0284, USA. E-mail: astra@ufl.edu*

surface exposed AAV2 tyrosine residues leads to ubiquitination and degradation of viral particles.[22] Site-directed tyrosine to phenylalanine (Y-F) mutagenesis of some of the seven capsid surface-exposed AAV2 tyrosine residues in the VP3 common region has been observed to result in the protection of vector particles from proteasome degradation and significant increases in the transduction efficiency of mutant vectors relative to the wild-type AAV2 vector both in tissue culture and in animals.[23] Another approach to alter capsid structure has employed shuffling of capsid gene sequences,[24] for example in generating recombinant AAVs with an increased ability to infect Müller cells.[25,26]

We recently showed that intraocular delivery of self-complementary AAV vectors-containing single-point Y-F mutations in some of the seven surface-exposed capsid tyrosine residues in AAV2, AAV8, or AAV9 led to significantly increased transduction efficiencies relative to their wild-type counterparts.[27] Although scAAV vectors bypass the need for conversion of the single-stranded AAV genome to double-stranded DNA, thus allowing for a faster and increased expression of the transgene of interest, their reduced packaging capacity represents a significant disadvantage for many gene-delivery applications. We therefore sought vector alternatives that avoided the need for self-complementary vector genomes for rapid, high efficiency retinal cell transduction.

Here, we examine the transduction characteristics of several conventional (nonself complementary) AAV2 vectors-containing various combinations of Y-F mutations in capsid surface-exposed tyrosine residues following subretinal or intravitreal delivery in adult mice. We report that the multiply mutated vectors exhibited different *in vivo* transduction properties, with some having a unique ability to express the transgene in all retinal layers following a single injection on either side of the retina. The potential to transduce photoreceptors and even some RPE cells, the targets of most inherited retinal degenerations, following intravitreal vector delivery may allow avoidance of surgically traumatic subretinal injections currently necessary to transduce these cell types.

RESULTS

Because single phenylalanine (F) for tyrosine (Y) substitutions had increased the potency of AAV2 following intraocular injections,[27] we analyzed green fluorescent protein (GFP) expression from viruses containing multiple combinations of Y-F capsid mutations in adult mouse retinas with respect to effects on tropism and transduction efficiency relative to wild-type AAV2: two double (Y444,730F) and (Y704,730F), one triple (Y444,500,730F), one quadruple (Y272,444,500,730F), one pentuple (Y272,444,500,704,730F) one sextuple (Y252,272,444,500,704,730F), and one septuple (Y252,272,444,500,700,704,730F) mutant vectors. One micro liter (10^{10} total vector genomes) of wild-type AAV2-CBA-GFP or the tyrosine-mutants were delivered either to the subretinal or the vitreal space of adult mice. The surface locations of each targeted tyrosine residue on the AAV2 capsid are shown in **Figure 1**.

Behavior of subretinal multiple Y-F mutated AAV2 vectors

Fundoscopic imaging of living mice was used to monitor GFP expression following subretinal delivery of various multiple tyrosine-mutant vectors. Previous studies have shown that it takes about 6–8 weeks postinjection for AAV2-mediated gene expression to reach maximal levels in the retina.[17] At 3 weeks postinjection, the triple mutant (Y444,500,730F) virus led to intense and uniform expression of funduscopically detectable GFP fluorescence (**Figure 2a**). At this same time point, wild-type AAV2 and other Y-F mutants led to less intense or barely detectable fluorescence (data not shown). At 10 weeks postinjection, when GFP expression had reached a plateau, this difference remained (**Figure 2b–h**). Eyes treated with the triple mutant displayed widespread and intense fluorescence, stronger than wild type and all other Y-F mutants examined (**Figure 2d**). GFP expression in the eyes treated with the sextuple or septuple mutants showed much weaker fluorescence than triple (**Figure 2g,h**). Out of the double Y-F mutants tested, only the (Y444, 730F) showed a detectable GFP signal in fundus images (**Figure 2c**).

Transgene expression was analyzed in more detail by immunohistochemistry of frozen retinal sections (**Figure 3**). For subretinal delivery, in addition to the expected AAV2 pattern of photoreceptors and RPE transduction,[28] which occurred for all mutants, the sextuple vector (Y252,272,444,500,704,730F) also displayed an unusual ability to transduce all retinal layers including ganglion cells (**Figure 3e**). The images in **Figure 3** have been purposely overexposed to reveal the full details of expression patterns for each mutant. This unique pattern was also seen in pentuple (Y272,444,500,704,730F), and septuple (Y252,272,444,500,700,704,730F) mutant vector treated eyes, although to a lesser degree (**Figure 3d,f**). GFP fluorescence was widely distributed over the entire retina (**Supplementary Figure S1a**). GFP expression for all other mutants delivered subretinally, including the (Y444,500,730F) triple mutant, was confined primarily to the photoreceptors and RPE cells (**Figure 3b**), with a few inner retinal cells being transduced by the quadruple mutant (**Figure 3c**). In contrast to other vectors, some of the triple mutant-treated retinas displayed photoreceptor cell loss (thinning of the outer nuclear layer) and an absence of outer segments (**Supplementary Figure S1b**). This apparently toxic effect may be related to the triple mutant's very high levels of GFP expression, which may lead to photoreceptor dysfunction. That only the triple Y-F mutant showed this effect is consistent with it being the most potent for expressing its transgene in photoreceptors (see above). Moderate expression of GFP is not toxic to the rodent retina.[29] Some of the inner retinal neurons transduced by the quadruple and pentuple mutants are rod bipolar cells, as identified by immunolabeling with a protein kinase C antibody (**Figure 4a,b**). Extensive bipolar cell transduction has not been previously observed following subretinal injection of AAV. Similarly, we also observed productive infection of retinal ganglion cells (RGCs) following subretinal injection. Extensive colocalization of GFP with Tuj-1, a ganglion cell marker, confirms that subretinal pentuple and sextuple mutants transit the entire retinal thickness and transduce ganglion cells (**Figure 4c,d**).

Behavior of intravitreal multiple Y-F mutated AAV2 vectors

GFP expression in the eyes treated intravitreally with various tyrosine mutants was initially analyzed by immunohistochemistry of retinal flatmounts to quantitatively evaluate the RGC transduction ability for each vector 1 month postinjection. At this time

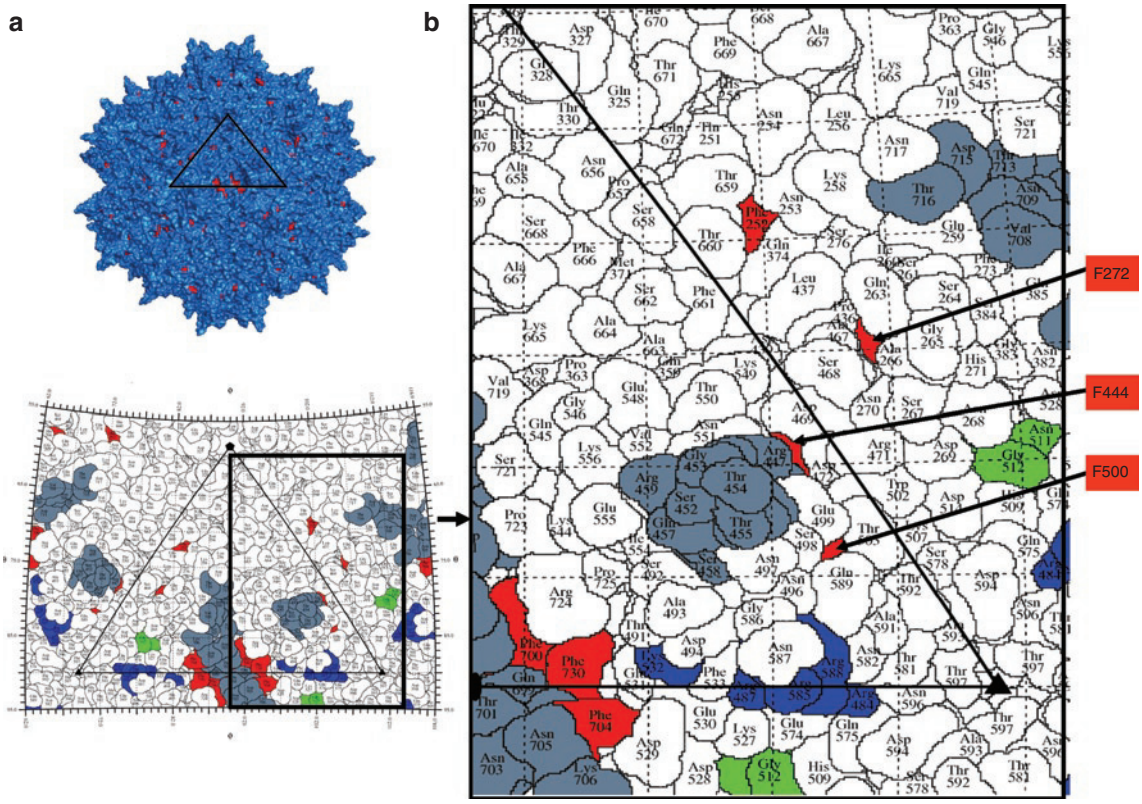

Figure 1 Distribution of mutated tyrosine residues (depicted in red) on the AAV2 capsid surface. (**a**) Molecular model of the complete AAV2 capsid assembled from 60 VP3 monomers generated with the Pymol software (www.pymol.org). (**b**) A "roadmap" showing the position of the mutated tyrosine residues (red), heparan sulfate binding sites (blue), NGR motif (green) known to bind the α5β1 coreceptor, and neutralizing peptides residues (gray) on the surface of the AAV2 capsid. An icosahedral viral asymmetric unit is depicted by the large triangle bounded by two threefold axes (filled triangles) separated by a twofold axis (filled oval) and a fivefold (filled pentagon). A close-up view is shown to the right. This figure was produced with the RIVEM program.[50] Note that mutated residues 700, 704, and 730 are located close to the positively charged residues involved in the interaction with the heparan sulfate receptor, and tyrosines 700 and 704 are part of a neutralizing epitope region.[32] AAV2, adeno-associated virus serotype 2.

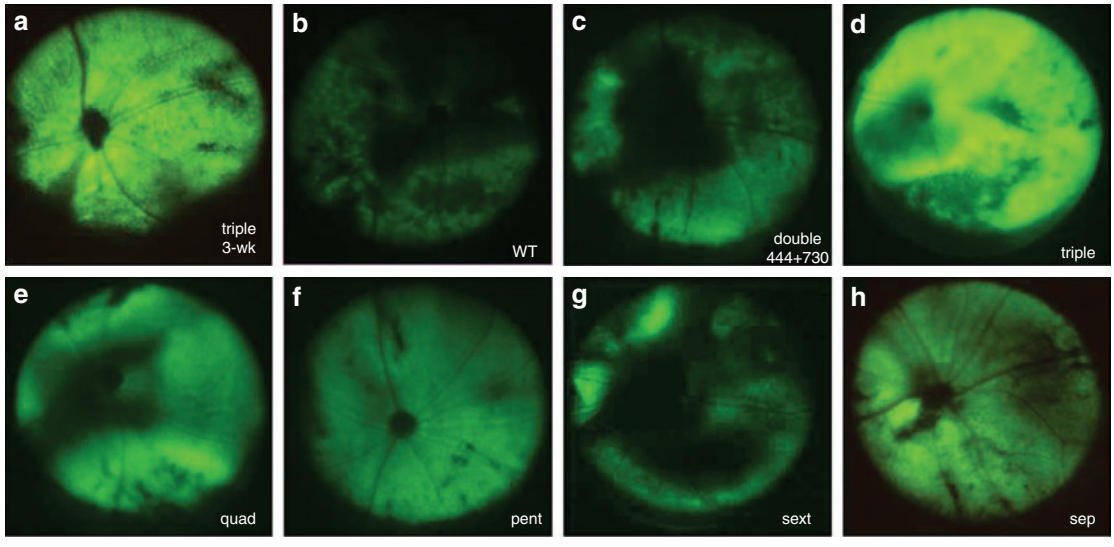

Figure 2 Representative fundus photographs showing GFP expression *in vivo* after subretinal delivery of multiple Y-F mutant AAV2 vectors in adult mouse retinas. (**a**) Strong fluorescence was detectable as early as 3 weeks postinjection in eyes treated with the (Y444,500,730F) triple mutant, and remained higher for this mutant (**d**) than for other vectors at 10 weeks postinjection, (**b**) AAV2 wild type, (**c**) double mutant (Y444, 730F), (**e**) quadruple mutant (Y272,444,500,730F), (**f**) pentuple mutant (Y272,444,500,704,730F), (**g**) sextuple mutant (Y252,272,444,500,704,730F), (**h**) septuple mutant (Y252,272,444,500,700,704,730F). AAV2, adeno-associated virus serotype 2; GFP, green fluorescent protein.

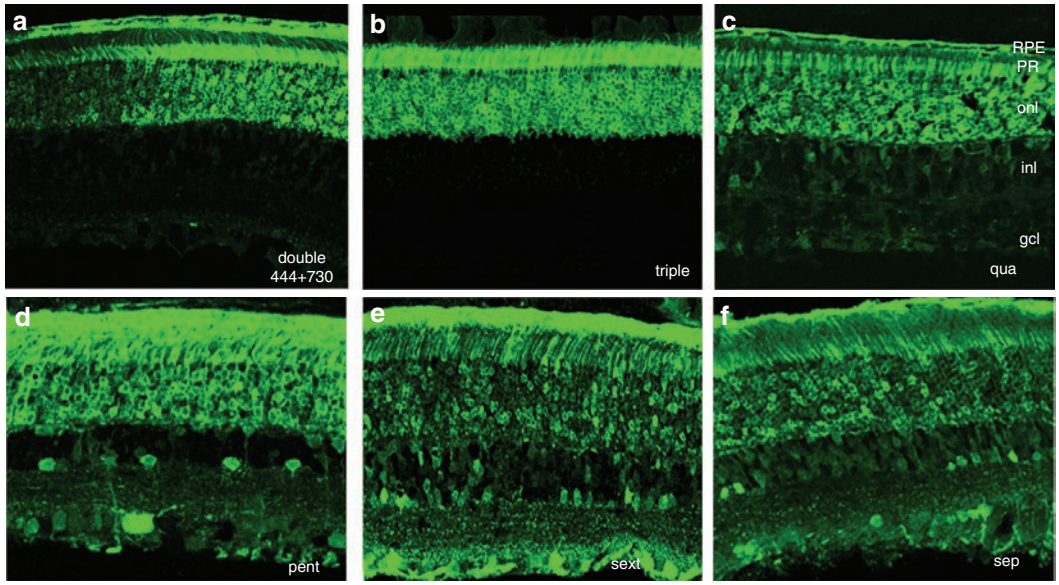

Figure 3 Representative images of GFP expression in retinal sections by immunohistochemistry at 1 month after subretinal vector injection with: (**a**) double mutant (Y444,730F), (**b**) triple mutant (Y444,500,730F), (**c**) quadruple mutant (Y272,444,500,730F), (**d**) pentuple mutant (Y272,444,500,704,730F), (**e**) sextuple mutant (Y252,272,444,500,704,730F), and (**f**) septuple mutant (Y252,272,444,500,700,704,730F). Images were intentionally overexposed to allow for visualization of all transduced inner retinal cells. AAV2, adeno-associated virus serotype 2; gcl, ganglion cell layer; GFP, green fluorescent protein; inl, inner nuclear layer; onl, outer nuclear layer; PR, photoreceptor layer; rpe, retinal pigmented epithelium.

point, the triple mutant was the only one that displayed significantly increased transduction efficiency relative to wild type, with intense labeling of RGCs and their axons (**Figure 5**).

In view of the unique transduction properties of some of the Y-F vectors when injected subretinally, we also studied their behavior 1 month after intravitreal delivery in wild-type mice by immunostaining of frozen retinal sections (**Figure 6**). In this case, all mutants shared a similar pattern of GFP expression in the ganglion, Müller, and inner retinal cells (**Figure 6**). However, the quadruple and pentuple Y-F mutant vectors also led to uniform GFP expression through the entire thickness of the retina, even extending to some RPE cells. It is important to note that the extensive transduction of the outer retina and occasional areas of RPE cells were only seen by using the highest titer vectors, those of at least 1×10^{13} genome copies/ml. When virus was delivered at tenfold lower titer (1×10^{12} genome copies/ml), GFP fluorescence was observed predominantly in ganglion, Müller cells, and inner retina (**Supplementary Figure S2a**). Even at this lower titer, fluorescence was consistently seen uniformly distributed over the entire retina (**Supplementary Figure S2b**). GFP expression was found to colocalize with calretinin, a marker of a subset of ganglion and amacrine cells, in addition to being present in the characteristic multiple strata of RGC dendritic arbors within the inner plexiform layer (**Figure 7a**). Bipolar cell targeting from these mutants at 1 month after intravitreal delivery was revealed using protein kinase C-α immunostaining in retinal sections (**Figure 7b,d**). We estimate that some of the Y-F mutant serotypes described above were able to increase bipolar cell transduction by at least fourfold when compared to the wild-type vector, suggesting their potential use for targeting these cells in a degenerated retina that may have lost the majority of its photoreceptors.

In order to evaluate outer retinal transduction using a cell-specific promoter following intravitreal delivery, an identical capsid quadruple mutant AAV2 containing a murine rhodopsin promoter-Gfp cassette was delivered at the same titer (1×10^{13} genome copies/ml) as the above vectors. The use of this weaker but photoreceptor specific promoter also produced widespread fluorescence in photoreceptor cells throughout the retina (**Supplementary Figure S2c**).

DISCUSSION

The data presented in this article show that mutagenesis of multiple critical surface-exposed tyrosine residues on AAV2 capsids can alter the transduction efficiency, kinetics, and perhaps the penetration ability of the virus when delivered to the retina. Although conventional single-stranded recombinant AAV2 vectors are able to transduce a variety of retinal cell types including photoreceptors, RPE, and ganglion cells following either a subretinal or intravitreal approach,[28,30] they do not efficiently infect cells of the inner retina except occasionally near the site of injection, and it usually takes weeks for wild-type vector to reach maximal, steady-state levels of transgene expression. Another disadvantage of wild-type AAV2 is the frequently seen antibody-mediated immunity against its capsid, which may prevent transgene expression in the contralateral eye following vector readministration, depending on the route of delivery.[31] Thus, pre-existing AAV2 neutralizing antibodies in a potential patient may preclude inclusion in a gene therapy protocol. These drawbacks could potentially be overcome by the use of capsid tyrosine mutants of AAV. For example, tyrosines 700 and 704 are part of a neutralizing epitope region comprising residues 697–716 on AAV2 capsid.[32] Because all the highly conserved tyrosine residues described in this work

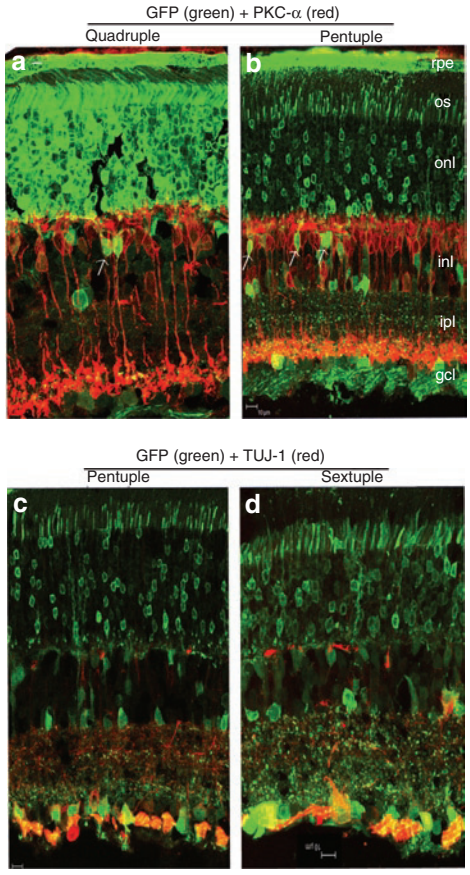

Figure 4 Detection of vector-expressed GFP in rod bipolar or ganglion cells in frozen retinal sections by immunohistochemistry at 1 month following subretinal injections with different AAV2 Y-F mutant vectors. (**a**,**b**) Arrows indicate colocalization of GFP (green) and PKC-α positive rod bipolar cells (red) in the retinas treated with the quadruple and pentuple mutant, respectively; (**c**,**d**) Colocalization of GFP (green) with TUJ-1 positive (red) ganglion cells for pentuple and sextuple mutant-treated retinas. Bar = 10 µm. AAV2, adeno-associated virus serotype 2; gcl, ganglion cell layer; GFP, green fluorescent protein; ipl, inner plexiform layer; inl, inner nuclear layer; onl, outer nuclear layer; os, outer segment; rpe, retinal pigment epithelium.

are located within the C-terminal common region of VP3, their mutation to phenylalanine affects the entire surface of the AAV2 capsid, potentially altering its interaction with cellular receptors, intracellular trafficking to the nucleus, and host immune recognition (see **Figure 1**). The unique architecture of the retina containing multiple neuronal layers adds an interesting dimension to the AAV transduction properties. Thus, even though all Y-F vectors described here shared a similar transduction pattern with the wild type, targeting mainly the RPE and photoreceptors after subretinal delivery, or ganglion cells following the intravitreal route, some mutants displayed unique properties, including a significantly higher transduction efficiency for inner neurons, or transduction of cell types separated from the injection site by multiple layers of intervening retinal cells.

Changing just three tyrosine (Y) residues on the AAV2 capsid as in the triple mutant (Y444,500,730F) to nonphosphorylatable phenylalanine (F) residues enhances intravitreally delivered vector transduction efficiency in ganglion cells by >30-fold (see **Figure 5**). It has recently been shown that simultaneous conversion of tyrosines 444, 500, and 730 to phenylalanine increases transgene expression in murine hepatocytes significantly, by potentially rendering the viral particles less prone to ubiquitination and proteasomal degradation, and the same phenomenon may contribute to the increased photoreceptor and ganglion cell transduction of this triple mutant vector in the retina.[33,34] In some eyes, triple mutant treatment caused significant photoreceptor cell loss following subretinal delivery, suggesting that it is not always beneficial to overexpress large amounts of protein in some neuronal cells,[35] and the choice of weaker, cell-specific promoters may be critical for future therapeutic applications. This toxic effect was most likely due to GFP overexpression rather than the vector itself, since the other, less potent multiple Y-F mutant vectors did not cause similar degeneration. Previous studies have also reported this phenomenon when using a high-titer AAV preparation in combination with a strong promoter.[36]

Interestingly, an increase in the number of tyrosine mutations beyond the three at 444, 500, and 730 did not further enhance transduction efficiency for either photoreceptors or ganglion cells,

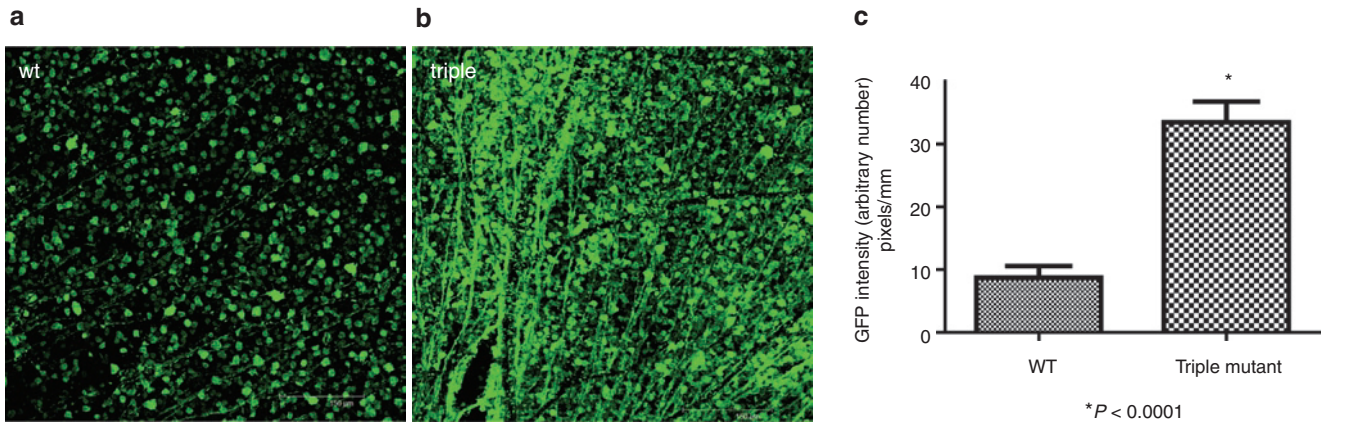

Figure 5 Immunohistochemistry for GFP protein expression in flat-mount whole retinas at 1 month following intravitreal delivery. (**a**) WT AAV2, (**b**) triple mutant (Y730,500,444F), (**c**) Comparison of GFP intensity of wild-type AAV2 vector and triple mutant in retinal flatmounts. Values indicate percent GFP intensity relative to treatment with wild-type AAV2 vector. All pictures were taken with the same exposure time to evaluate GFP intensity using ImageJ. AAV2, adeno-associated virus serotype 2; GFP, green fluorescent protein; WT, wild type.

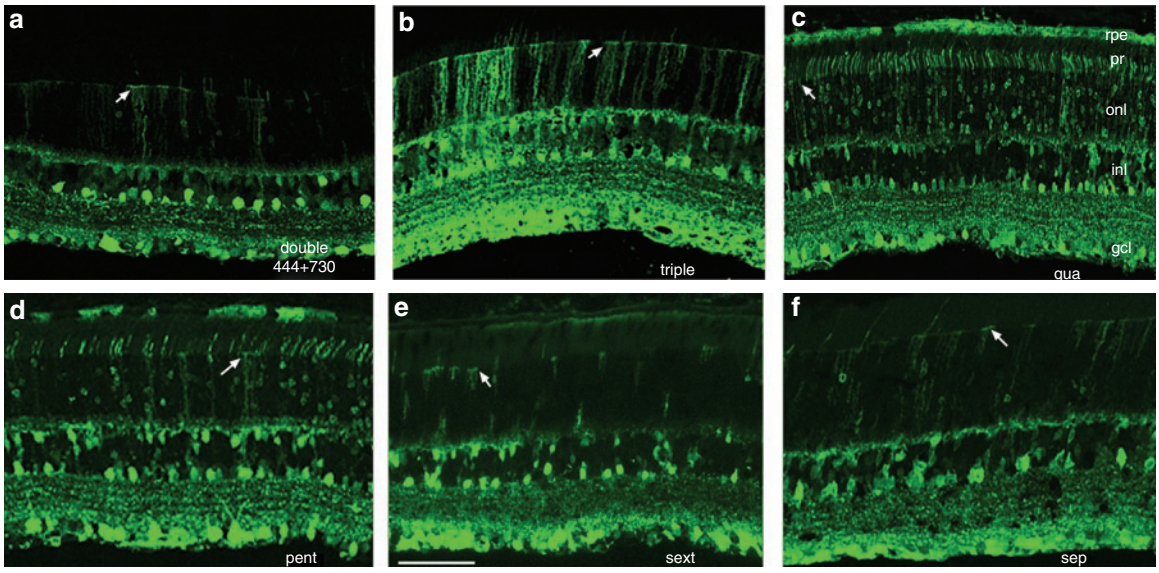

Figure 6 Immunostaining for GFP protein expression in retinal sections at 1 month following intravitreal delivery of (a) double mutant (Y444,730F), (b) triple mutant (Y730,500,444F), (c) quadruple mutant (Y272,444,500,730F), (d) pentuple mutant (Y272,444,500,704,730F), (e) sextuple mutant (Y252,272,444,500,704,730F), and (f) septuple mutant (Y252,272,444,500,700,704,730F). Note the GFP expression throughout all retinal layers with the quadruple and pentuple mutant, and intense labeling of Müller cell outward processes terminating at the outer limiting membrane (arrows), in all mutants analyzed. Bar = 100 µm. AAV2, adeno-associated virus serotype 2; gcl, ganglion cell layer; GFP, green fluorescent protein; inl, inner nuclear layer; onl, outer nuclear layer; PR, photoreceptor layer; rpe, retinal pigmented epithelial layer.

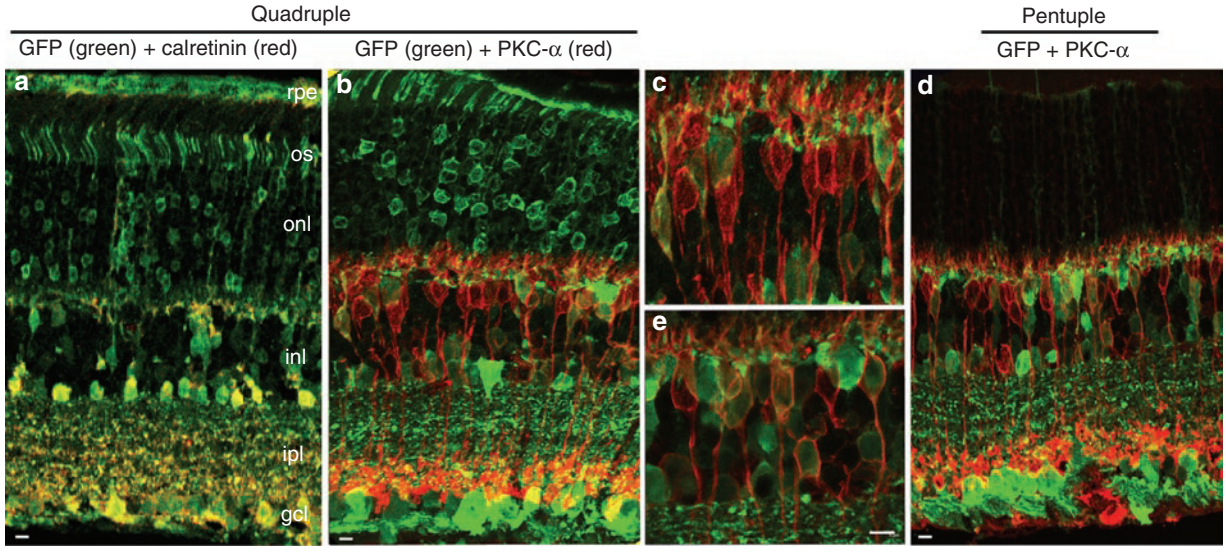

Figure 7 Evaluation of colocalization of GFP (green) with cell-marker proteins (red), as shown by immunohistochemistry of frozen retinal sections at 1 month following intravitreal injections with different AAV2 Y-F mutant vectors in adult mice. (**a**) Colocalization (yellow) of GFP and some calretinin (red) positive ganglion or amacrine cells after injection of the quadruple mutant. (**b**,**d**) Colocalization of GFP (green) and PKC-α (red) positive rod bipolar in the eyes treated with the quadruple or pentuple mutant vector, respectively; (**c**,**e**) Insets of panels (**b**) and (**d**) at higher magnification showing colocalization of GFP and PKC-α in the inner nuclear layer. Bar = 10 µm (**a**;**b**;**d**) and 5 µm (**c**;**e**). AAV2, adeno-associated virus serotype 2; gcl, ganglion cell layer; GFP, green fluorescent protein; ipl, inner plexiform layer; inl, inner nuclear layer; onl, outer nuclear layer; os, outer segments; rpe, retinal pigmented epithelial layer.

but clearly led to more widespread GFP expression in multiple retinal layers, including, in some cases, those layers located distal from the injection site. For example, mutagenesis of six exposed tyrosines on the AAV2 capsid led to transduction of many inner retinal cells following subretinal delivery and a relatively uniform GFP expression even in RGCs. One possible explanation for this property may be related to the extracellular interactions required for vector binding to the cell surface, subsequent capsid entry, or intracellular events following internalization. Mutating an increasing number of tyrosine residues, located in polar hydrophilic environments on the capsid surface, to phenylalanine residues, would be expected to increase the hydrophobicity of the capsid surface. Additionally, residues 700, 704, and 730 are located close to a positively charged patch of amino acids comprising the heparan

sulfate-binding region on the AAV2 capsid surface (shown in **Figure 1**). It is possible that simultaneous modification of these residues alters AAV2 interaction with its primary heparan sulfate receptor, thus reducing its affinity for photoreceptors, and allowing the potentially more hydrophobic virus particles to penetrate more efficiently toward the ganglion cell layer. It should also be noted that trans-synaptic transport of AAV particles between neurons through an anterograde or retrograde manner has been proposed as a mechanism to permit transgene expression over a wide area.[37–40] Although axonal transport, known to be dependent on the capsid structure,[40] may play a role in the behavior of some Y/F mutants, it cannot account for the transduction of RPE cells from vitreal vector because there are no synapses connecting retinal cells with the RPE.

The transduction ability of mutant vectors was different depending on the delivery route, and this behavior may have been influenced by the cellular barriers the virus encountered in each approach, subretinal or intravitreal. Thus, while the sextuple mutant led to GFP expression across the entire retina after subretinal delivery, it infiltrated less efficiently following the intravitreal route, as no RPE cells and very few photoreceptors were GFP^+ in this case. One recent study has shown enhanced penetration and transduction of all retinal layers by wild-type AAV following mild digestion of the inner limiting membrane with a nonspecific protease,[41] suggesting that the retinal intercellular matrix limits penetration of intravitreally delivered vectors. Thus, an inner limiting membrane barrier adjacent to vitreally delivered vector may serve to limit transduction of cells in distal retinal layers, whereas it would play no such role in limiting subretinal vector penetration. A combination of mechanisms may contribute to retinal cell transduction across multiple layers. As discussed above, some of the Y/F mutants may differ from each other and the wild type with respect to their tissue penetration potential. Thus, after subretinal delivery, the triple mutant would be expected to transduce the ganglion cells the most efficiently if it were able to reach them at the same frequency as other, less potent vectors, such as the sextuple. Accordingly, while the subretinal triple mutant was extremely efficient for photoreceptor transduction, suggesting many vector particles were bound there, few other retinal cells were transduced. This in turn suggests that the sextuple mutant, being less efficient at binding to and transducing photoreceptors, may have a potentially larger penetration potential than the triple upon subretinal delivery. In the case of intravitreal vector, while the diffusion of a larger number of mutant AAV2 particles from the vitreous to the outer retina cannot be entirely ruled out, an alternative and not mutually exclusive interpretation of the distribution of GFP expression is that because multiple Y-F mutants transduce cells efficiently, we can detect their presence in the interneurons at a lower effective particle number. Previous studies have shown that although wild type AAV2 preferentially targets ganglion cells after intravitreal delivery, it also transduces Müller glia, amacrine and occasional bipolar and photoreceptor cells.[28,42] Thus, the widespread GFP expression which becomes apparent in all these cell types following intravitreal Y-F vector, may stem simply from an enhancement of the pre-existing wild-type AAV2 potential to target these cells under similar experimental conditions along with the ability of each mutant to intracellular escape from proteasomal degradation. More studies will be needed to precisely elucidate the role of each conserved tyrosine residue in the biology of AAV2 in the retina. We note that such unique transduction properties of mutated AAV vectors which allow transgene expression to be expressed over large distances in living tissue might enhance the utility of these vectors for the treatment of solid tumors.[43]

Unlike Leber congenital amaurosis type 2 caused by RPE65 mutations, in which photoreceptor cell loss occurs at a relatively slow rate, disorders characterized by a fast onset of retinal degeneration, for example retinal detachment,[44,45] could benefit from the availability of vectors that possess either an enhanced ability to transduce the outer retina via intravitreal delivery, or a faster kinetics and higher transduction efficiency in photoreceptors cells. Intravitreal delivery is known to be considerably less invasive by avoiding the necessarily traumatic side effects of retinal detachment associated with subretinal vector injection. Because the majority of retinal disorders are caused by mutations in either photoreceptors or RPE cells, administration of these vectors from the vitreal side of the retina would present a distinct surgical safety advantage, particularly in those cases in which an underlying genetic defect leads to a degenerative process and a fragile retina, prone to further damage upon surgically induced retinal detachment. Remarkably, for some mutant vectors, such as the quadruple, almost every retinal cell type appears to have been transduced following the intravitreal approach. This may be a distinct advantage in many late-stage retinal diseases when all photoreceptors are lost. For example, Y-F mutant AAV-mediated expression of microbial-type channel rhodopsins, such as ChR2, in surviving retinal neurons may represent a viable approach for restoring some light sensitivity in patients with no photoreceptor preservation due to advanced retinal degeneration.[46,47] Although the efficiency of photoreceptor transduction following subretinal delivery remains higher than the intravitreal option, according to a recent study[48] the transduction potential from intravitreal vector may increase in a diseased retina, due to an elevated penetration of AAV particles from the vitreous toward the outer nuclear layer in damaged retinas. As noted above, it may be advantageous to have the option of delivering low levels of transgenes to mutant photoreceptors, avoiding potential toxic effects related to overexpression of an otherwise therapeutic protein.

In conclusion, novel multiple-Y-F mutant AAV2 vectors exhibit properties in the retina that suggest valuable options for potentially safer and more effective treatment of a wide variety of retinal diseases requiring therapeutic gene delivery. Future studies will address the mechanisms by which some of these mutant AAVs lead to widespread transgene expression transiting the entire retina following a single treatment.

MATERIALS AND METHODS

Production of recombinant AAV2 vectors. Site-directed mutagenesis of surface-exposed tyrosine residues on AAV2 VP3 was performed as previously described.[23] Vector preparations were produced by the plasmid co-transfection method as shown previously.[49] Briefly, the crude iodixanol fraction, was further purified and concentrated by column chromatography on a 5-ml HiTrap Q Sepharose column using a Pharmacia AKTA FPLC system (Amersham Biosciences, Piscataway, NJ). The vector was eluted from the column using 215 mM NaCl, pH 8.0, and the vector containing

fractions collected, pooled, concentrated, and buffer exchanged into Alcon BSS with 0.014% Tween 20, using a Biomax 100 K concentrator (Millipore, Billerica, MA). The titer of DNase-resistant vector genomes was measured by real-time PCR relative to a standard. Finally, the purity of the vector was validated by silver-stained sodium dodecyl sulfate–polyacrylamide gel electrophoresis, assayed for sterility and lack of endotoxin, and then aliquoted and stored at −80 °C.

Intraocular administration of vector. Only adult C57BL/6 mice were used in this study. All animals were maintained in the University of Florida Health Science Center in the animal care facilities under a 12/12 hours light/dark environment, and were handled in accordance with the ARVO statement for Use of Animals in Ophthalmic and Vision Research and the guidelines of the Institutional Animal Care and Use Committee at the University of Florida. Before vector administration, mice were anesthetized with ketamine (72 mg/kg)/xylazine (4 mg/kg) by intraperitoneal injection. Wild-type AAV2 or the tyrosine-mutants were delivered either to the subretinal or the intravitreal space of adult mice, as previously described.[27] One hour before the anesthesia, the eyes were dilated with one drop of 1% atropine, followed by topical administration of 2.5% phenylephrine. An aperture within the pupil was made through the cornea with a 30 1/2-gauge disposable needle and a 33-gauge unbeveled blunt-tip needle on a Hamilton syringe was introduced through the corneal opening into the subretinal space. For Intravitreal injections, a 33-gauge beveled needle was passed through the sclera, at the equator, next to the *limbus*, into the vitreous. Each eye received 1 µl of vector at a titer of 1×10^{13} genome copies/ml.

Fundus photography. Fundus images were captured every week after injection for up to 10 weeks, using a Kowa Genesis digital camera connected to a dissecting microscope after anesthetizing the animals and dilating their pupils as above.

Preparation of retinal flat mounts and cryosections. At 1 month after vector injection, mice were humanely euthanized, the eyes removed and fixed with 4% paraformaldehyde in phosphate-buffered saline for 1 hour and the cornea and lens then removed. To make flat mounts, the entire retina was carefully dissected from the eyecup and radial cuts were made from the edges to the equator of the retina. For cryosections, the eyecups were washed in phosphate-buffered saline followed by immersion in 30% sucrose in the same buffer overnight. Eyes were then embedded in optimal cutting temperature embedding compound (Miles Diagnostics, Elkhart, IN) and oriented for 10-µm thick transverse retinal sections.

Immunolabeling and histological analysis. Flat-mounted retinas were incubated with 0.5% Triton X-100 for 1 hour followed by incubation with a blocking solution of 0.5% Triton X-100 and 1% bovine serum albumin for 1 hour. Retinas were incubated with a commercial mouse monoclonal antibody raised against the GFP (Invitrogen, Molecular Probes, Carlsbad, CA) at 1:400 dilution in blocking solution overnight at room temperature in a slow orbital shaker. Tissue sections were incubated with 0.5% Triton X-100 for 15 minutes, then washed three times with phosphate-buffered saline for 5 minutes each, followed by incubation with a blocking solution of 1% albumin for 30 minutes. The sections were incubated with the same mouse monoclonal antibody against GFP at 1:400 dilution overnight at 37 °C. A mouse anti-β3 tubulin (TUJ-1; Covance, Richmond, CA), protein kinase C-α (mouse sc8393), and calretinin (sc135853) from Santa Cruz Biotechnology (Santa Cruz Biotechnology, Santa Cruz, CA) were used for colocalization experiments. Retinal flatmounts and sections were examined by fluorescence microscopy using a Leica TCS SP2 Laser Scanning confocal microscope (Leica, Heidelberg, Germany). GFP staining intensity in flat mounts was quantified from fluorescence microscopic images using ImageJ (National Institutes of Health) software to determine the fluorescence intensity in pixels per unit area. Differences between groups were evaluated with GraphPad Prism software (GraphPad, La Jolla, CA) using one-way ANOVA followed by Dunnett's post-test for group comparison.

SUPPLEMENTARY MATERIAL

Figure S1. Immunostained retinal sections of GFP expression at 1 month after subretinal delivery.

Figure S2. Immunostained retinal sections of GFP expression at 1 month after intravitreal delivery.

ACKNOWLEDGMENTS

We acknowledge the National Institutes of Health grants EY11123, EY13729, EY07132, EY08571, EY11087, EY0667, EY018335, NS36302, HL59412 (MAM) and grants from Foundation Fighting Blindness, Macular Vision Research Foundation, Research to Prevent Blindness, Inc. and CNPq for partial support to this work. We thank Doug Smith, Tom Doyle, Min Ding, Song Mao, Thomas Andresen, and Todd A. Barnash for technical assistance. W.W.H. and the University of Florida have a financial interest in the use of AAV therapies, and own equity in a company (AGTC Inc.) that might, in the future, commercialize some aspects of this work.

REFERENCES

1. Daya, S and Berns, KI (2008). Gene therapy using adeno-associated virus vectors. *Clin Microbiol Rev* **21**: 583–593.
2. Mueller, C and Flotte, TR (2008). Clinical gene therapy using recombinant adeno-associated virus vectors. *Gene Ther* **15**: 858–863.
3. Cideciyan, AV, Aleman, TS, Boye, SL, Schwartz, SB, Kaushal, S, Roman, AJ *et al.* (2008). Human gene therapy for RPE65 isomerase deficiency activates the retinoid cycle of vision but with slow rod kinetics. *Proc Natl Acad Sci USA* **105**: 15112–15117.
4. Bainbridge, JW, Smith, AJ, Barker, SS, Robbie, S, Henderson, R, Balaggan, K *et al.* (2008). Effect of gene therapy on visual function in Leber's congenital amaurosis. *N Engl J Med* **358**: 2231–2239.
5. Hauswirth, WW, Aleman, TS, Kaushal, S, Cideciyan, AV, Schwartz, SB, Wang, L *et al.* (2008). Treatment of leber congenital amaurosis due to RPE65 mutations by ocular subretinal injection of adeno-associated virus gene vector: short-term results of a phase I trial. *Hum Gene Ther* **19**: 979–990.
6. Maguire, AM, Simonelli, F, Pierce, EA, Pugh, EN Jr, Mingozzi, F, Bennicelli, J *et al.* (2008). Safety and efficacy of gene transfer for Leber's congenital amaurosis. *N Engl J Med* **358**: 2240–2248.
7. Xie, Q, Bu, W, Bhatia, S, Hare, J, Somasundaram, T, Azzi, A *et al.* (2002). The atomic structure of adeno-associated virus (AAV-2), a vector for human gene therapy. *Proc Natl Acad Sci USA* **99**: 10405–10410.
8. Bleker, S, Sonntag, F and Kleinschmidt, JA (2005). Mutational analysis of narrow pores at the fivefold symmetry axes of adeno-associated virus type 2 capsids reveals a dual role in genome packaging and activation of phospholipase A2 activity. *J Virol* **79**: 2528–2540.
9. Summerford, C and Samulski, RJ (1998). Membrane-associated heparan sulfate proteoglycan is a receptor for adeno-associated virus type 2 virions. *J Virol* **72**: 1438–1445.
10. Kern, A, Schmidt, K, Leder, C, Müller, OJ, Wobus, CE, Bettinger, K *et al.* (2003). Identification of a heparin-binding motif on adeno-associated virus type 2 capsids. *J Virol* **77**: 11072–11081.
11. Opie, SR, Warrington, KH Jr, Agbandje-McKenna, M, Zolotukhin, S and Muzyczka, N (2003). Identification of amino acid residues in the capsid proteins of adeno-associated virus type 2 that contribute to heparan sulfate proteoglycan binding. *J Virol* **77**: 6995–7006.
12. Akache, B, Grimm, D, Pandey, K, Yant, SR, Xu, H and Kay, MA (2006). The 37/67-kilodalton laminin receptor is a receptor for adeno-associated virus serotypes 8, 2, 3, and 9. *J Virol* **80**: 9831–9836.
13. Asokan, A, Hamra, JB, Govindasamy, L, Agbandje-McKenna, M and Samulski, RJ (2006). Adeno-associated virus type 2 contains an integrin α5β1 binding domain essential for viral cell entry. *J Virol* **80**: 8961–8969.
14. Kashiwakura, Y, Tamayose, K, Iwabuchi, K, Hirai, Y, Shimada, T, Matsumoto, K *et al.* (2005). Hepatocyte growth factor receptor is a coreceptor for adeno-associated virus type 2 infection. *J Virol* **79**: 609–614.
15. Qing, K, Mah, C, Hansen, J, Zhou, S, Dwarki, V and Srivastava, A (1999). Human fibroblast growth factor receptor 1 is a co-receptor for infection by adeno-associated virus 2. *Nat Med* **5**: 71–77.
16. Summerford, C, Bartlett, JS and Samulski, RJ (1999). αVβ5 integrin: a co-receptor for adeno-associated virus type 2 infection. *Nat Med* **5**: 78–82.
17. Natkunarajah, M, Trittibach, P, McIntosh, J, Duran, Y, Barker, SE, Smith, AJ *et al.* (2008). Assessment of ocular transduction using single-stranded and self-complementary recombinant adeno-associated virus serotype 2/8. *Gene Ther* **15**: 463–467.
18. Zincarelli, C, Soltys, S, Rengo, G and Rabinowitz, JE (2008). Analysis of AAV serotypes 1-9 mediated gene expression and tropism in mice after systemic injection. *Mol Ther* **16**: 1073–1080.
19. Davidoff, AM, Gray, JT, Ng, CY, Zhang, Y, Zhou, J, Spence, Y *et al.* (2005). Comparison of the ability of adeno-associated viral vectors pseudotyped with serotype 2, 5, and 8 capsid proteins to mediate efficient transduction of the liver in murine and nonhuman primate models. *Mol Ther* **11**: 875–888.
20. Broekman, ML, Comer, LA, Hyman, BT and Sena-Esteves, M (2006). Adeno-associated virus vectors serotyped with AAV8 capsid are more efficient than AAV-1 or -2 serotypes

for widespread gene delivery to the neonatal mouse brain. *Neuroscience* **138**: 501–510.
21. Wu, Z, Asokan, A and Samulski, RJ (2006). Adeno-associated virus serotypes: vector toolkit for human gene therapy. *Mol Ther* **14**: 316–327.
22. Zhong, L, Li, B, Jayandharan, G, Mah, CS, Govindasamy, L, Agbandje-McKenna, M *et al.* (2008). Tyrosine-phosphorylation of AAV2 vectors and its consequences on viral intracellular trafficking and transgene expression. *Virology* **381**: 194–202.
23. Zhong, L, Li, B, Mah, CS, Govindasamy, L, Agbandje-McKenna, M, Cooper, M *et al.* (2008). Next generation of adeno-associated virus 2 vectors: point mutations in tyrosines lead to high-efficiency transduction at lower doses. *Proc Natl Acad Sci USA* **105**: 7827–7832.
24. Maheshri, N, Koerber, JT, Kaspar, BK and Schaffer, DV (2006). Directed evolution of adeno-associated virus yields enhanced gene delivery vectors. *Nat Biotechnol* **24**: 198–204.
25. Koerber, JT, Klimczak, R, Jang, JH, Dalkara, D, Flannery, JG and Schaffer, DV (2009). Molecular evolution of adeno-associated virus for enhanced glial gene delivery. *Mol Ther* **17**: 2088–2095.
26. Klimczak, RR, Koerber, JT, Dalkara, D, Flannery, JG and Schaffer, DV (2009). A novel adeno-associated viral variant for efficient and selective intravitreal transduction of rat Müller cells. *PLoS ONE* **4**: e7467.
27. Petrs-Silva, H, Dinculescu, A, Li, Q, Min, SH, Chiodo, V, Pang, JJ *et al.* (2009). High-efficiency transduction of the mouse retina by tyrosine-mutant AAV serotype vectors. *Mol Ther* **17**: 463–471.
28. Auricchio, A, Kobinger, G, Anand, V, Hildinger, M, O'Connor, E, Maguire, AM *et al.* (2001). Exchange of surface proteins impacts on viral vector cellular specificity and transduction characteristics: the retina as a model. *Hum Mol Genet* **10**:3075–3081.
29. Daniels, DM, Shen, WY, Constable, IJ and Rakoczy, PE (2003). Quantitative model demonstrating that recombinant adeno-associated virus and green fluorescent protein are non-toxic to the rat retina. *Clin Experiment Ophthalmol* **31**: 439–444.
30. Martin, KR, Klein, RL and Quigley, HA (2002). Gene delivery to the eye using adeno-associated viral vectors. *Methods* **28**: 267–275.
31. Li, Q, Miller, R, Han, PY, Pang, J, Dinculescu, A, Chiodo, V *et al.* (2008). Intraocular route of AAV2 vector administration defines humoral immune response and therapeutic potential. *Mol Vis* **14**: 1760–1769.
32. Moskalenko, M, Chen, L, van Roey, M, Donahue, BA, Snyder, RO, McArthur, JG *et al.* (2000). Epitope mapping of human anti-adeno-associated virus type 2 neutralizing antibodies: implications for gene therapy and virus structure. *J Virol* **74**: 1761–1766.
33. Li, M, Jayandharan, GR, Li, B, Ling, C, Ma, W, Srivastava, A *et al.* (2010). High-Efficiency Transduction of Fibroblasts and Mesenchymal Stem Cells by Tyrosine-Mutant AAV2 Vectors for Their Potential Use in Cellular Therapy. *Hum Gene Ther* (epub ahead of print).
34. Markusic, DM, Herzog, RW, Aslanidi, GV, Hoffman, BE, Li, B, Li, M *et al.* (2010). High-efficiency Transduction and Correction of Murine Hemophilia B Using AAV2 Vectors Devoid of Multiple Surface-exposed Tyrosines. *Mol Ther* (epub ahead of print).
35. Klein, RL, Dayton, RD, Leidenheimer, NJ, Jansen, K, Golde, TE and Zweig, RM (2006). Efficient neuronal gene transfer with AAV8 leads to neurotoxic levels of tau or green fluorescent proteins. *Mol Ther* **13**: 517–527.
36. Beltran, WA, Boye, SL, Boye, SE, Chiodo, VA, Lewin, AS, Hauswirth, WW *et al.* (2010). rAAV2/5 gene-targeting to rods:dose-dependent efficiency and complications associated with different promoters. *Gene Ther* **17**: 1162–1174.
37. Provost, N, Le Meur, G, Weber, M, Mendes-Madeira, A, Podevin, G, Cherel, Y *et al.* (2005). Biodistribution of rAAV vectors following intraocular administration: evidence for the presence and persistence of vector DNA in the optic nerve and in the brain. *Mol Ther* **11**: 275–283.
38. Stieger, K, Colle, MA, Dubreil, L, Mendes-Madeira, A, Weber, M, Le Meur, G *et al.* (2008). Subretinal delivery of recombinant AAV serotype 8 vector in dogs results in gene transfer to neurons in the brain. *Mol Ther* **16**: 916–923.
39. Kaspar, BK, Erickson, D, Schaffer, D, Hinh, L, Gage, FH and Peterson, DA (2002). Targeted retrograde gene delivery for neuronal protection. *Mol Ther* ***5***: 50–56.
40. Cearley, CN and Wolfe, JH (2007). A single injection of an adeno-associated virus vector into nuclei with divergent connections results in widespread vector distribution in the brain and global correction of a neurogenetic disease. *J Neurosci* **27**: 9928–9940.
41. Dalkara, D, Kolstad, KD, Caporale, N, Visel, M, Klimczak, RR, Schaffer, DV *et al.* (2009). Inner limiting membrane barriers to AAV-mediated retinal transduction from the vitreous. *Mol Ther* **17**: 2096–2102.
42. Hellström, M, Ruitenberg, MJ, Pollett, MA, Ehlert, EM, Twisk, J, Verhaagen, J *et al.* (2009). Cellular tropism and transduction properties of seven adeno-associated viral vector serotypes in adult retina after intravitreal injection. *Gene Ther* **16**: 521–532.
43. Thorsen, F, Afione, S, Huszthy, PC, Tysnes, BB, Svendsen, A, Bjerkvig, R *et al.* (2006). Adeno-associated virus (AAV) serotypes 2, 4 and 5 display similar transduction profiles and penetrate solid tumor tissue in models of human glioma. *J Gene Med* **8**: 1131–1140.
44. Fisher, SK, Lewis, GP, Linberg, KA and Verardo, MR (2005). Cellular remodeling in mammalian retina: results from studies of experimental retinal detachment. *Prog Retin Eye Res* **24**: 395–431.
45. Arroyo, JG, Yang, L, Bula, D and Chen, DF (2005). Photoreceptor apoptosis in human retinal detachment. *Am J Ophthalmol* **139**: 605–610.
46. Tomita, H, Sugano, E, Isago, H, Hiroi, T, Wang, Z, Ohta, E *et al.* (2010). Channelrhodopsin-2 gene transduced into retinal ganglion cells restores functional vision in genetically blind rats. *Exp Eye Res* **90**: 429–436.
47. Lagali, PS, Balya, D, Awatramani, GB, Münch, TA, Kim, DS, Busskamp, V *et al.* (2008). Light-activated channels targeted to ON bipolar cells restore visual function in retinal degeneration. *Nat Neurosci* **11**: 667–675.
48. Kolstad, KD, Dalkara, D, Guerin, K, Visel, M, Hoffmann, N, Schaffer, D *et al.* (2009). Changes to AAV mediated gene delivery in retinal degeneration. *Hum Gene Ther* **21**: 571–578.
49. Zolotukhin, S, Byrne, BJ, Mason, E, Zolotukhin, I, Potter, M, Chesnut, K *et al.* (1999). Recombinant adeno-associated virus purification using novel methods improves infectious titer and yield. *Gene Ther* ***6***: 973–985.
50. Xiao, C and Rossmann, MG (2007). Interpretation of electron density with stereographic roadmap projections. *J Struct Biol* **158**: 182–187.